

Dissociative Photoionization of Iron Pentacarbonyl in the Range 38–120 eV

Yusuke Tamenori and Inosuke Koyano*

Department of Material Science, Himeji Institute of Technology, 1479-1 Kanaji, Kamigori 678-12, Japan

Received: July 7, 1997[⊗]

Dissociative photoionization processes of iron pentacarbonyl are investigated in the inner-valence region by use of the photoelectron–photoion coincidence (PEPICO) and photoion–photoion coincidence (PIPICO) technique combined with synchrotron radiation. Photon energy dependence of the yield is examined in detail for all observed ions and ion pairs in the range 38–120 eV. Ions observed in the PEPICO measurements include not only the fragment ions resulting from simple CO elimination but also those resulting from additional cleavage of the C–O covalent bond(s) in the ligand. In the PIPICO measurements, several novel ion pairs that unambiguously indicate the cleavage of the covalent C–O bond in the ligated state are detected. From the analysis of these PEPICO and PIPICO efficiency curves, dissociation mechanisms leading to all ions and ion pairs are discussed, placing special emphasis on the cleavage of one or more covalent C–O bonds. It is concluded that the increased extent of the back-donation of $d\pi$ electrons of the central metal atom to the $2\pi^*$ antibonding orbital of CO plays an important role in the C–O bond cleavage.

Introduction

The transition-metal carbonyls, especially iron pentacarbonyl, have long received considerable attention as a key species in organometallic reactions and homogeneous catalytic cycles. In particular, the coordinatively unsaturated species have been central to these studies because these compounds have been known to be the active agent in the above reaction systems. From the interest in these processes as well as the interest in its own right, a considerable number of experimental^{1–9} and theoretical^{10–12} studies have been performed on the stability and reactivity and the geometric and electronic structures of variously coordinated compounds. Sequential bond dissociation energies (BDEs) of the coordination bonds, both of neutral and ionic species, provide a set of key information on these properties, and thus their determinations have extensively been performed using various experimental techniques,^{1–9} especially for the monocation series.

The transition-metal carbonyls are also an interesting system for the study of molecular dissociation dynamics. The interest arises from the fact that these compounds have two distinct types of chemical bonds in a molecule: one the weak metal–ligand coordination bond (bond energy = a few electronvolts) and the other the strong C–O covalent bond (11.2 eV). However, the majority of previous studies on the dissociation processes, in the both neutral and ionized regime, concerned only with the scission of the metal–carbonyl coordination bonds, and only a few studies have concerned the processes involving the C–O bond scission.^{4,8,13} These latter studies in fact have demonstrated that a substantial fraction of dissociation products result from the C–O bond rupture when a sufficient energy is supplied. Thus, it is expected that studies of the competition between these two bond rupture processes as a function of the partitioned energy provide an opportunity to investigate some new aspects of these systems, such as intramolecular energy transfer through

the weak coordination and strong covalent bonds. This in turn may yield new information about the nature of the metal–carbonyl chemical bonds that cannot be obtained from the BDE measurements alone.

Such a sufficient energy is conveniently provided by photoexcitation or photoionization in the inner-valence or inner-shell region. The excitation of the inner-valence or inner-shell electrons has an additional advantage that it generally leads to more localized initial energy deposition. This contrasts with the excitation of valence electrons, which are delocalized over the molecule, and constitute a more favorable situation for the study of the intramolecular energy transfer. From these points of view, we have recently initiated a series of detailed studies of dissociative photoionization processes of metal carbonyl vapors in the inner-valence regions, using photoelectron–photoion coincidence (PEPICO) and photoion–photoion coincidence (PIPICO) techniques combined with synchrotron radiation.^{14–18} An emphasis is placed on the C–O bond rupture and the relationship between the electronic states and dissociation pathways. The present paper presents a full account of the results on the dissociative single, double, and triple photoionization of $\text{Fe}(\text{CO})_5$ studied in the photon energy region of 38–120 eV.¹⁵ Results on $\text{W}(\text{CO})_6$ ¹⁶ have appeared already,¹⁴ and those on $\text{Mo}(\text{CO})_6$ ¹⁷ and $\text{Cr}(\text{CO})_6$ ¹⁸ are forthcoming.

Information on the inner-valence excitation of iron pentacarbonyl comes from the studies of electron energy loss spectroscopy,¹⁹ photoelectron spectroscopy,²⁰ and ab initio calculation.²¹ These studies reported a strong absorption resonance at about 60 eV, which corresponds to the iron 3p–3d excitation. On the other hand, the studies of dissociation processes over a wide energy range have been performed by Winters et al.² and Heck et al.⁸ Winters et al., using a TOF mass spectrometry with electron impact ionization, measured the variation of the relative abundances of the $\text{Fe}(\text{CO})_n^+$ ($n = 0–5$) ions with the excitation energy, but they could not find fragment ions produced via cleavage of the C–O bond, nor the fragment ions having no metal atom. Heck et al., who studied

[⊗] Abstract published in *Advance ACS Abstracts*, December 15, 1997.

the dissociation processes in the range from 20 to 90 eV using TOF mass spectrometry and the PIPICO technique combined with synchrotron radiation, reported that no features were observed in the fragmentation patterns at the photon energy of the above-mentioned 3p–3d excitation.⁸ Their main interest was in the dissociation dynamics from the kinetic energy release distribution of fragment species. Although both studies were carried out in a rather wide energy range encompassing the inner-valence region, the number of measuring points (in terms of energy) used was not sufficient to reveal any structure corresponding to specific electronic states.

Experimental Section

All experiments in this study are carried out at the UVSOR synchrotron radiation facility in Okazaki. The apparatus used is that installed on the BL3A2 beamline. Details of the setup and experimental procedures have been described in previous reports.²² In this section, we outline the apparatus and the experimental procedure briefly.

Synchrotron radiation from 750 MeV electron storage ring is dispersed by a constant-deviation grazing incidence monochromator. The monochromatic photon beams are focused onto the center of the ionization cell containing sample gas. The produced ions and electrons are extracted from the ionization cell in opposite directions to each other by an electric field. The ions are then accelerated to a high energy and mass-analyzed by a double field type time-of-flight (TOF) mass spectrometer. The electric field in the first stage is adjusted between 187.5 and 375 V/cm to obtain best collecting efficiency, whereas that in the second stage is fixed at 3530 V/cm for all measurements. All measurements are carried out at the detection angle of 55° with respect to the polarization vector of the incident photon to minimize the effect of anisotropic angular distribution of photoions and photoelectrons. The sample gas pressure in the ionization cell is estimated to be $\sim 1 \times 10^{-6}$ Torr from the pressure in the main chamber housing the cell, which is kept at $(5-8) \times 10^{-7}$ Torr.

The mass spectrometer is used in two different modes of operation: photoelectron–photoion coincidence (PEPICO) and photoion–photoion coincidence (PIPICO) measurement modes. Photoionization mass spectra are obtained by the PEPICO mode. The procedure for this measurement is as follows. The photoelectrons, extracted from the ionization cell, are detected by a channel electron multiplier (CEM), and its output is fed into the start input of a time-to-amplitude converter (TAC). On the other hand, the photoions are detected at the end of the drift tube by a multichannel plate (MCP), and its output is fed into the stop input of the TAC. As the flight times of photoelectrons from the ionization cell to the electron detector are much shorter than those of photoions, the time-of-flight differences between the photoelectrons and photoions are essentially the flight times of photoions from the ionization cell to the detector.

The positive-ion pairs resulting from dissociative double and triple photoionization are identified in the PIPICO measurement mode. In this mode, the photoion signal generated at the detector first is fed into the start input and that generated second is fed into the stop input of the TAC. In this way, the pairs of ions originating from a single molecule are identified from their TOF differences.

The liquid sample Fe(CO)₅ are degassed by repeating several freeze–pump–thaw cycles with liquid N₂ prior to measurement. The sample is contained in a Pyrex glass tubing, which is wrapped in aluminum foil to protect the sample from undesirable light.

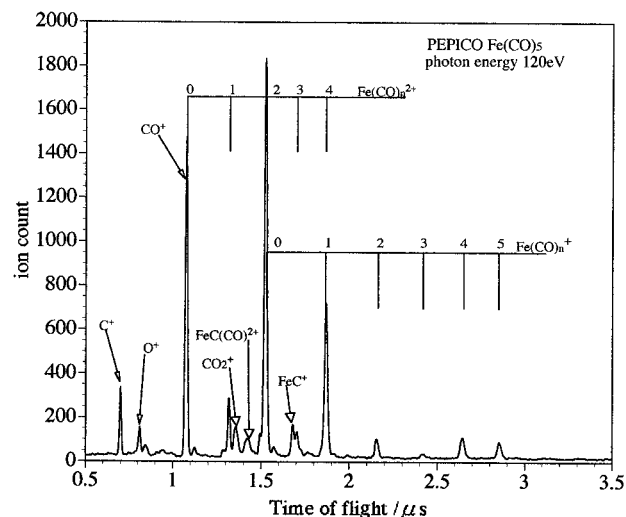


Figure 1. PEPICO (TOF) spectrum of Fe(CO)₅ taken at 120 eV of incident photon energy with 41 cm of drift tube length.

Results and Discussion

PEPICO Measurement. Figure 1 shows an example of TOF mass spectrum of Fe(CO)₅ taken at 120 eV of incident photon energy and with 20.0 cm flight path length. As can be seen, the most abundant ions are those corresponding to the formula Fe(CO)_n⁺ ($n = 0-5$) and CO⁺, all of which are produced by simple scission of (a) metal–carbonyl coordination bond(s) in a singly and/or multiple charged ions. If we recall that the covalent C–O bond is much stronger than that of the metal–carbonyl coordination bond, this result sounds reasonable. It can also be seen that doubly charged ions of the formula Fe(CO)_n²⁺ ($n = 0-4$) are formed as well, with lifetimes longer than a few microseconds.

It should be noted here that some ambiguity exists concerning the mass identification in the present system, because the mass of Fe (56) is exactly twice the mass of CO (28). Namely, the m/z values of some dications containing Fe coincide with that of a monocation with different number of CO. Specifically, the assignments given above to Fe(CO)_n²⁺ with $n =$ even number, Fe(CO)_n⁺ with $n = 0$ and 1, and CO⁺ cannot be conclusive owing to this mass coincidence. For example, the two highest peaks ($m/z = 56$ and 28) could be a composite of Fe⁺ and Fe(CO)₂²⁺ and of CO⁺ and Fe²⁺, respectively. However, from the results on other metal carbonyl systems, such as M(CO)₆ ($M = \text{Cr, Mo, W}$),^{14,16-18} we can safely conjecture that the Fe(CO)₂²⁺ dication has a large abundance and the Fe²⁺ dication has a small abundance. The reason is as follows. As can be seen in Figure 1, the intensities of the peaks corresponding to Fe⁺/Fe(CO)₂²⁺ ($m/z = 56$) and CO⁺/Fe²⁺ ($m/z = 28$) are high and comparable with each other. However, in the PEPICO spectra of other metal carbonyls, the peak of CO⁺ is generally by far the most intense among others. Also, it is generally found that among monocation fragments of the form M(CO)_n⁺ the most abundant species is the naked metal ion M⁺ ($n = 0$), whereas among dication fragments most abundant ions are those having some carbonyls still left on the metal; naked metal dications M²⁺ are seldom observed. With all these facts combined, it may be concluded that CO⁺ is predominantly responsible for the $m/z = 28$ peak with little contribution coming from Fe²⁺, while both Fe⁺ and Fe(CO)₂²⁺ contribute substantially to the $m/z = 58$ peak.

Several interesting features are seen in the PEPICO spectrum. First, the relative abundance of the Fe(CO)₃⁺ ion is exceptionally small among monocations of the formula Fe(CO)_n⁺, in agree-

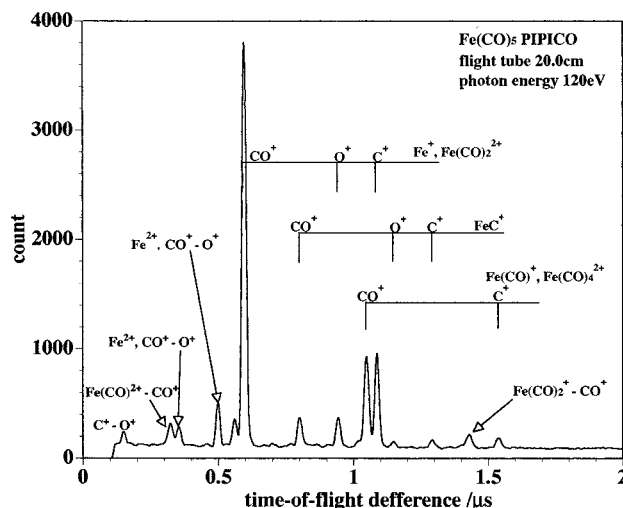


Figure 2. PIPICO spectrum of $\text{Fe}(\text{CO})_5$ taken under the same conditions as in the PEPICO spectrum in Figure 1.

ment with previous reports.²⁻⁵ In this connection, it is interesting to note that dication $\text{Fe}(\text{CO})_3^{2+}$ seems to exist, although the overlapping with the neighboring peak makes its clear identification difficult. Second, ions that definitely indicate the occurrence of the fission of the covalent C–O bond in the ligated state (without breaking weaker coordination bond) are observed, although their abundances are much smaller than those of the dominant ions mentioned above. These include FeC^+ and $\text{FeC}(\text{CO})^{2+}$. Third, the CO_2^+ fragment ions are observed, indicating that a drastic rearrangement occurs before and/or during the fragmentation of the parent ion. Finally, the observation of C^+ is also worthy of special attention because it evidently indicates the simultaneous breakage of the coordination Fe–C and covalent C–O bonds in one of the ligands.

PIPICO Measurement. Figure 2 shows an example of the PIPICO spectrum, which was taken under the same conditions as in the PEPICO spectrum shown in Figure 1. Again, several novel features are seen in this spectrum. The first is that the charge separative dissociation involving the fission of the covalent C–O bond is unambiguously demonstrated (observation of coincident ion pairs FeC^+-O^+ , FeC^+-C^+ , and $\text{Fe}(\text{CO})^+-\text{C}^+$). The second is that the dissociation of triply charged ions into dication–monocation pairs is observed, although metastable triply charged ions are not observed in the PEPICO spectrum. A conclusive evidence for such a process is given by the $\text{CO}^+-\text{Fe}(\text{CO})^{2+}$ coincidence peak. Unfortunately, however, all other peaks assignable to a dication–monocation pair are exactly overlapped by a peak corresponding to a monocation–monocation coincidence. The third feature is the observation of the pairs of ions having no metal atom, i.e., C^+-O^+ , C^+-CO^+ , and O^+-CO^+ . Although we do not have any detailed information as to how these ion pairs are formed, we pay special attention to them in this paper. Two possible origins would be (1) breakage of two covalent C–O bonds and (2) charge separative fragmentation from a triply charged ion into three singly charged ions. Finally, it is particularly interesting to note that the fragment ion FeC^+ , which must be produced in a process involving a C–O bond scission in the ligand (i.e., not in dissociated free CO^+), gives coincidence not only with O^+ and CO^+ but also with C^+ . In order for the coincidence between FeC^+ and C^+ to occur, scission of at least two C–O bonds is required: one in a ligated state and the other either in another ligand or in a dissociated free CO^+ state.

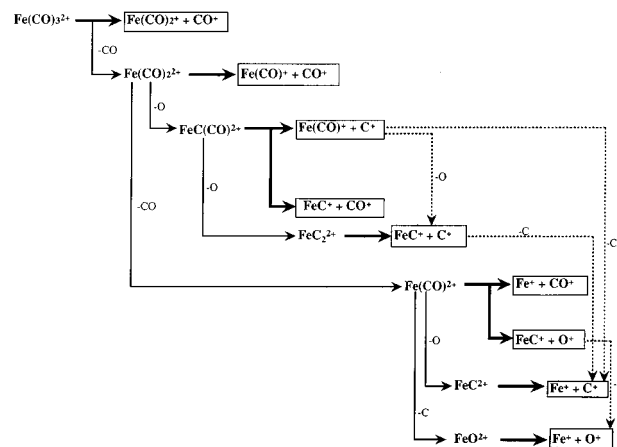
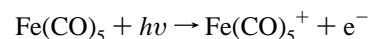


Figure 3. Entire scheme of dissociation pathways for doubly charged ions.

The observed positive ion pairs are summarized in Figure 3 (boxed), together with possible dissociation pathways leading to them (solid lines). Several of the pathways may gain firm support from the observation of the precursor (metastable) doubly charged ions in the PEPICO spectrum (bold solid lines), but others can only be a result of speculation (thin solid line). For the PIPICO peaks corresponding to Fe^+-C^+ , Fe^+-O^+ , and FeC^+-C^+ , for example, the precursor species may reasonably be speculated to be FeC_2^{2+} , FeO_2^{2+} , and FeC_2^{2+} , respectively. However, no such ions are found in the PEPICO spectrum. These ion pairs are evidently produced through breakage of one or more covalent C–O bonds. A consideration of detailed sequences of the decay processes would be of great help in identifying these precursors. This problem is discussed in detail in the next section in conjunction with the branching ratios.

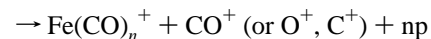
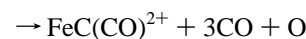
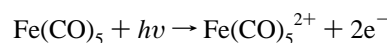
PEPICO and PIPICO Branching Ratios. Figure 4 shows plots of the ratios of the integrated intensities of the various PEPICO peaks to the total PEPICO intensity, as a function of the incident photon energy. From these curves, it is found that the photon energy region around 42 eV is very important in terms of the fragmentation involving the cleavage of the covalent C–O bond. In the region below 42 eV, the produced ions are mainly those corresponding to the formula $\text{Fe}(\text{CO})_n^+$, which are formed via simple CO elimination from the parent ions.



The only ion that evidently indicates the occurrence of the covalent C–O bond breakage is FeC^+ , whose appearance energy has been determined by Winters and Kiser at 22.1 eV.²



On the other hand, in the photon energy range above about 42 eV, the relative abundances of the ions $\text{Fe}(\text{CO})_n^+$ gradually decrease with the increase in the incident photon energy. Instead, the dications of the formulas $\text{Fe}(\text{CO})_n^{2+}$ and $\text{FeC}(\text{CO})^{2+}$ as well as monocations C^+ , O^+ , and CO^+ rapidly increase.



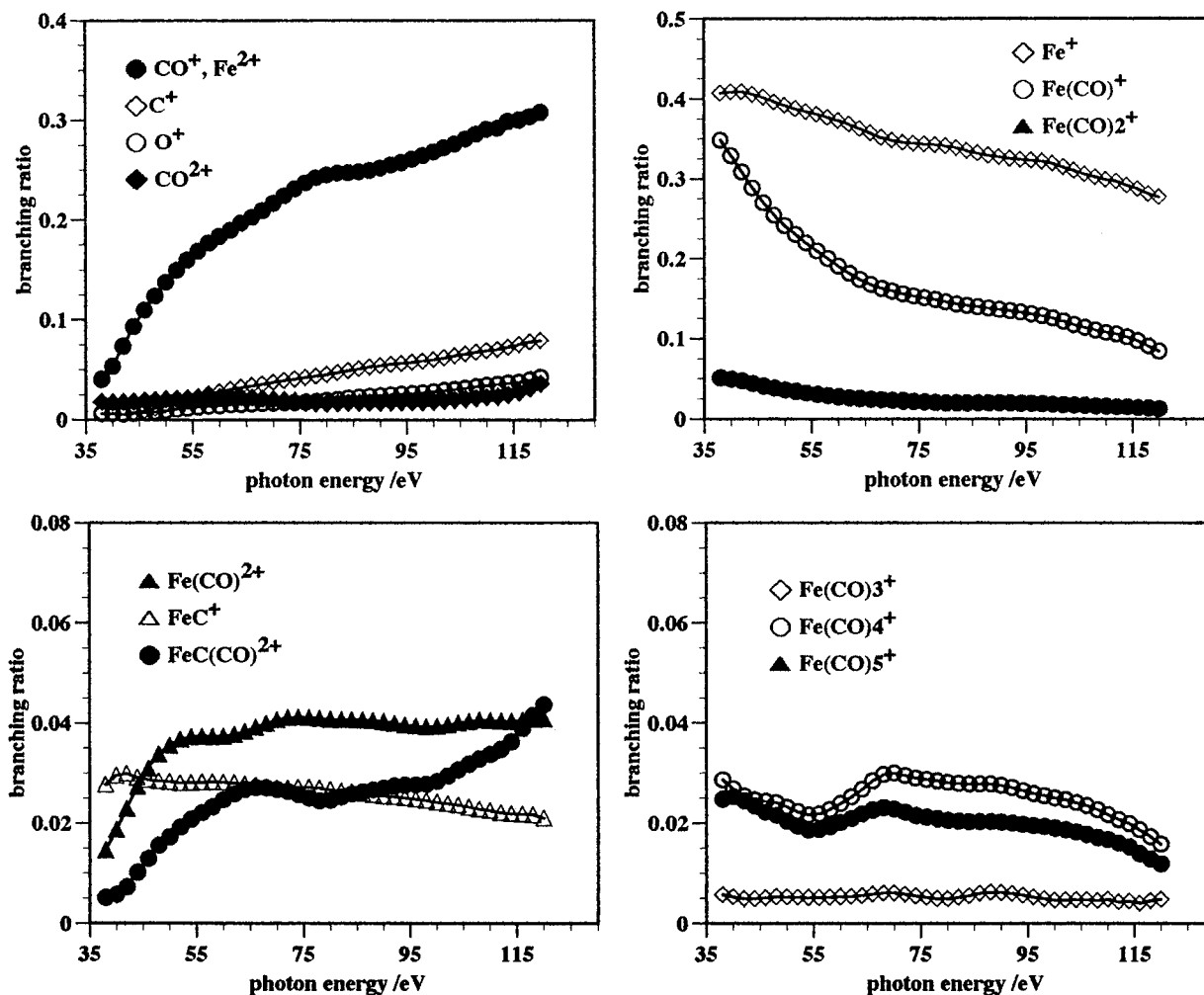


Figure 4. PEPICO branching ratios of $\text{Fe}(\text{CO})_5$ as a function of incident photon energy.

Here, np denotes the neutral products associated with each pair of ionic species. It is especially noteworthy that the ions having no metal atom are produced dominantly in this energy region. These ions must be produced by the charge separative dissociation of doubly and triply charged parent ions. A firm support for this statement comes from the PIPICO measurements carried out as a function of incident photon energy. Figure 5 shows the PIPICO branching ratios for various ion pairs in the range from 38 to 120 eV obtained by the same analysis as in the PEPICO measurement. Several ion pairs are seen to rise sharply at about 42 eV. All of these rising ion pairs involve as the lighter species an ion having no metal atom. Apparently, the increase in the dissociation into these ion pairs is responsible for the increase of ions having no metal atom in the PEPICO branching ratios.

The lack of the C^+ and O^+ fragment as well as the very weak intensity of CO^+ in the lower photon energy region indicates an interesting fact that the intramolecular charge transfer from the central metal atom to the ligand occurs extensively. Cooper et al. measured the relative photoionization cross section of transition-metal hexacarbonyl compounds in the incident photon energy range from 16 to 115 eV²³ and determined the photoelectron branching ratios of three valence bands (the metal d, CO $1\pi 5\sigma$, and CO 4σ bands in the range from 6 to 20 eV). The results indicated that the branching ratios of CO $1\pi 5\sigma$ and CO 4σ bands amount to about 60% and from 10% to 30%, respectively, in the whole energy range. In other words, the photoionization cross section of the metal d band is much

smaller than that of the CO bands. Judging from these results on hexacarbonyls, we can assume that the initial positive hole is mainly created in the ligand in the photoionization of $\text{Fe}(\text{CO})_5$ as well. Nevertheless, we could not detect the C^+ and O^+ fragments and find only a weak intensity of CO^+ in the range below 42 eV. This fact indicates that the positive charge created in the ligands of the parent monocation stays on the central metal atom when dissociating. In other words, a hole created in the ligand is quickly filled by electron outflow from the central metal atom. This may be rationalized by the lower ionization potential of the metal atom than that of CO. This electron flow assumption may also be applied to the double photoionization in the range above 42 eV. This stems from the fact that the observed fragment ions having no metal atom are only singly charged species (i.e., C^+ , O^+ , and CO^+), although the used photon energies are sufficient for the production of C^{n+} , O^{n+} , and CO^{n+} ($n \geq 2$). This observation is similar to the results obtained in the photoinitiated desorption study of chemisorbed CO on the metal surface.²⁴ The unique feature in the latter study has been interpreted in terms of the screening of the photoinduced hole by electron transfer from the substrate into the lowest unoccupied orbital of CO, which is $2\pi^*$. The details of this charge transfer is discussed below.

Roles of Double Photoionization in a Ligand and Metal 3p–3d Inner-Valence Excitation. The branching ratios in both measurements show a large variation in the inner-valence region. The relative abundances of the ions C^+ , O^+ , CO^+ , $\text{FeC}(\text{CO})_2^+$, and various ion pairs start to increase sharply above about 42

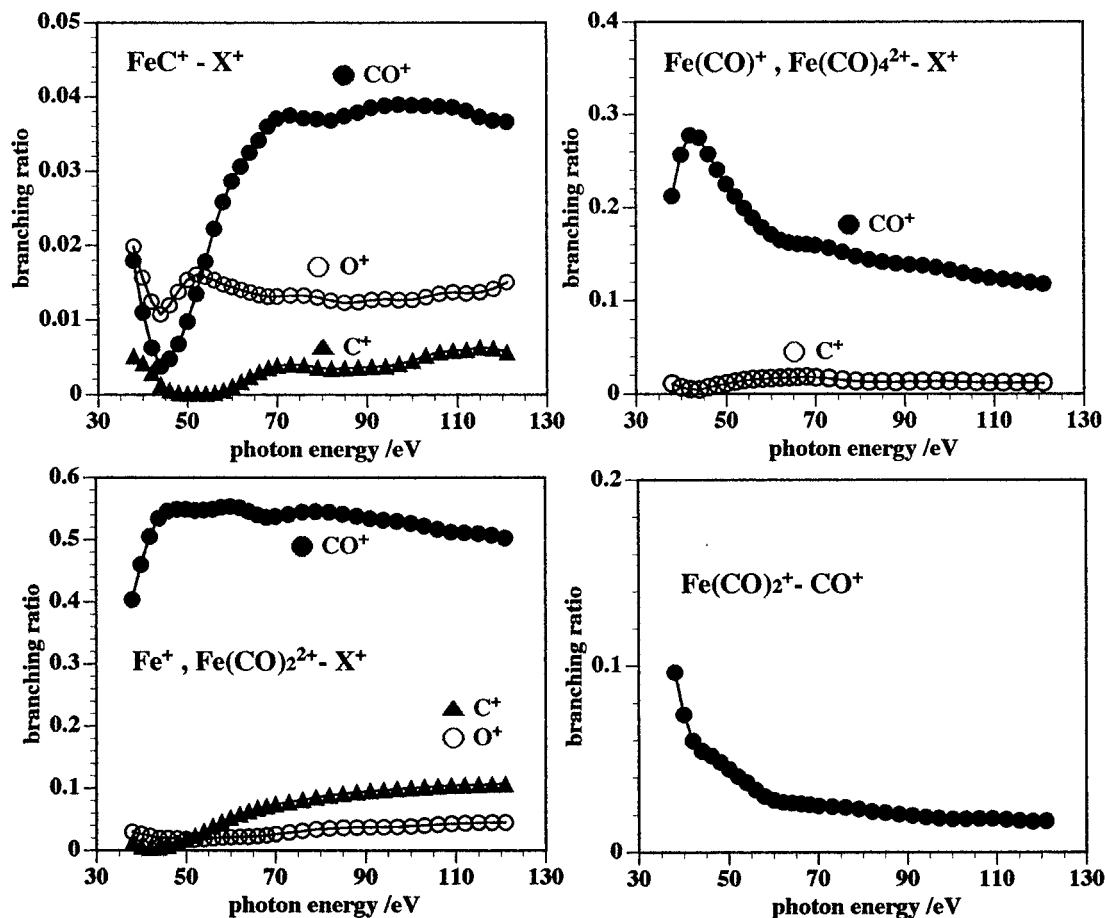
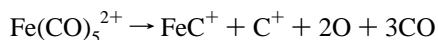


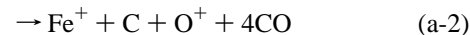
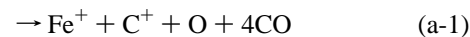
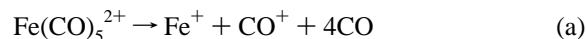
Figure 5. PIPICO branching ratios of $\text{Fe}(\text{CO})_5$ as a function of incident photon energy.

eV. This energy region includes the double photoionization threshold of CO, suggesting that the cleavage of the covalent C–O bond with charge separation is closely related to the double photoionization within the ligand. On the other hand, from the PIPICO branching ratio curves, another interesting photon energy region is found. That is the region above about 60 eV, where the peak corresponding to $\text{FeC}^+ - \text{C}^+$ appears.

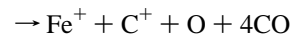
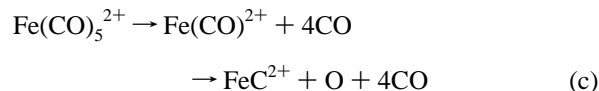
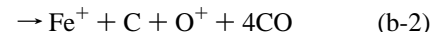
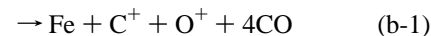
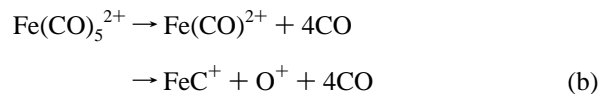


This ion pair can only be produced through the scission of two C–O covalent bonds. This energy region corresponds to the $3p \rightarrow 3d$ photoabsorption limit of Fe.^{19–21} Heck et al. claimed that no selective fragmentation is observed in this energy region.⁸ However, we find a dramatic variation in the branching ratios of some ions and ion-pairs around this energy. Such a variation is observed not only in this study but also in the same measurements for the hexacarbonyl compounds at the $np \rightarrow nd$ photoabsorption region.^{14,16–19} The excitation energy dependence reported by Winters et al., who paid attention only to the $\text{Fe}(\text{CO})_n^+$ ions, also did not show any specific variation in this energy region.² Our observations indicate that the metal $np \rightarrow nd$ photoabsorption and perhaps the double photoionization in one of the CO ligands cause the above specific fragmentation. The difference in the dissociation processes between the low and high photon energy regions is most conspicuously manifested in the fragment ions having no metal atom in the PEPICO spectrum and in several ion pairs in the PIPICO spectrum. Thus, the studies of these ions (C^+ , O^+ , CO^+ , and $\text{FeC}(\text{CO})_2^{2+}$) and the relevant ion pairs are essential to understand the dissociation dynamic of this compounds.

In examining the products originating from the cleavage of the covalent C–O bond in further detail, we have to distinguish two types of the C–O bond-breaking processes. One is the C–O bond breakage in a free CO^+ state:



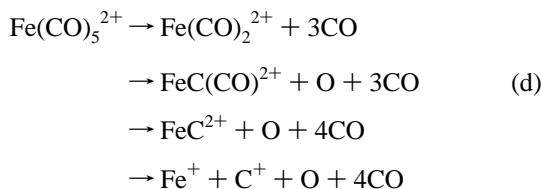
and the other that in a ligated state, most probably in $\text{Fe}(\text{CO})_2^{2+}$:



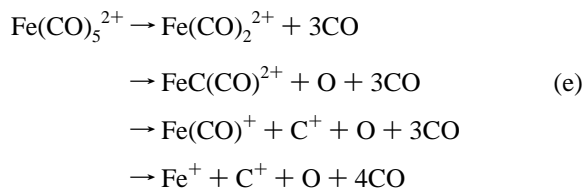
The dissociation pathways denoted by (b) show the C–O bond cleavage on the metal atom with charge separation, whereas those denoted by (c) show the case in which neutral O atom is eliminated from the dication. If the C–O bond is ruptured exclusively in free CO^+ after the charge separation process (a), almost the same intensities are expected for C^+ and O^+ , since Masuoka and Nakamura have shown that for the dissociation

of free CO^+ the ion branching ratios for C^+ and O^+ are almost the same over a wide energy range [equal probability for (a-1) and (a-2)].²⁵ However, our observed ion branching ratios of C^+ are twice as large as those of O^+ . The dominance of the C–O bond rupture in the free dication CO^{2+} is also ruled out based on the same experimental fact. Therefore, we have to consider some other dissociation mechanism(s) in which oxygen atoms are predominantly or exclusively ejected as neutral species. Such a mechanism must be the one involving the C–O bond breakage in the ligated state. The only possibility of such a process is process (c) considered above. The charge separative C–O bond breakage [process (b)] is ruled out simply because it would give an O^+ branching ratio either equal to or greater than that of C^+ , depending on the relative importance of the two subsequent fragmentation processes of FeC^+ , (b-1) and (b-2). That process (b) can be ruled out gains further support from the PIPICO results. If process (b) is the dominant process responsible for the C–O bond breakage, the ion pair $\text{O}^+ - \text{FeC}^+$ and/or other ion pairs $\text{O}^+ - \text{X}$, where X is an ion resulting from further fragmentation of FeC^+ , are expected to have large branching ratios. This, however, is not the case; instead, the dominant ion pair that is enhanced in this energy region is $\text{Fe}^+ - \text{C}^+$.

Thus, taking all these experimental findings into consideration, the dominant dissociation pathways involving the C–O bond breakage may be concluded to be process (c). It should be noted, however, that although we have considered so far only the C–O bond breakage process starting from dication $\text{Fe}(\text{CO})_2^{2+}$, similar neutral O atom elimination in the ligated state prior to charge separation is also possible starting from $\text{Fe}(\text{CO})_2^{2+}$, as shown in Figure 3. In fact, the dication $\text{Fe}(\text{CO})_2^{2+}$ is one of the species observed with moderate intensity, as can be seen in Figures 1 and 4. Thus, alternative dissociation pathways involving C–O bond breakage in the ligated state could be



or



Both of these pathways eventually lead to the same products and explain the enhanced $\text{Fe}^+ - \text{C}^+$ ion pair. However, we cannot distinguish between them from our experimental results alone and conclude at this stage that the dominant pathway(s) leading to the C–O bond rupture is (are) either (c), (d), or (e), or more than one of them. The essence of these mechanisms is that the C–O bond fission preferentially occurs in the ligated state rather than in free CO^+ and/or CO^{2+} and that the eliminated species is the neutral O atom rather than the O^+ ion.

Electronic Mechanism of the Covalent C–O Bond Breakage. An important finding in the present study is that the dissociation products relevant to the cleavage of the covalent C–O bond(s) (ions and ion-pairs) appear or are enhanced at

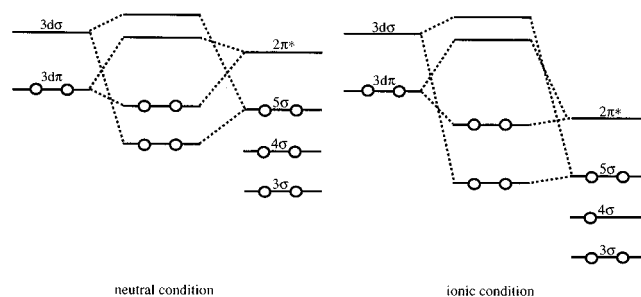


Figure 6. Scheme of intramolecular electron transfer from metal atom to CO ligand following initial ionization in the ligand.

the Fe $3p \rightarrow 3d$ threshold and the threshold for the double ionization of the CO ligand. Considering this observation together with the fact that the initial positive holes are predominantly created in the ligand,²³ we can formulate a qualitative model that explains the above observations consistently. The model, which is based on the intramolecular electron transfer from metal to ligand(s), is presented here.

First we give a simple picture of this electron transfer in relation to the donor–acceptor interaction model for the metal–carbonyl coordination bond in general. The metal–carbonyl bond is characterized by the hybridization of the CO 5σ and $2\pi^*$ orbitals with metal d orbitals; CO 5σ electron partially flows into a metal unoccupied orbital, and metal d electron partially flows into the CO antibonding orbital $2\pi^*$. The former is called the σ -donation interaction and the latter the π -back-donation interaction. The simple qualitative picture of this electron flow is illustrated in Figure 6 in terms of the relevant molecular orbitals. In the neutral ground state (left diagram), the bonding orbital involved in the π -back-donation interaction has a strong metal d character because of the lower energy of the metal d orbital than that of CO $2\pi^*$. However, in the ionized state (right diagram) having a positive hole in the ligand, the CO $2\pi^*$ character prevails over the metal d character in the π -back-donation orbital, since the CO $2\pi^*$ orbital becomes lower in energy than the metal d orbital due to the increased Coulomb attraction from the nuclei. This is nothing but the electron transfer from metal d to CO $2\pi^*$ orbital upon ionization. The final state is thus regarded as a ligated metal cation in which one of the CO ligands is in the excited state. This electron transfer is just in line with the π -back-donation interaction in coordination compounds.

Applying this model to the double photoionization within a ligand, the enhancement of the C–O bond breakage at this threshold is readily understood. The orbital energy of CO $2\pi^*$ is even more lowered in the doubly ionized molecule than in the singly ionized molecule due to the stronger Coulomb attraction from the nuclei (less shielded positive charge). This endows the π -back-donation orbital with more increased CO $2\pi^*$ character, meaning that still more metal d electrons flow into the CO $2\pi^*$ orbital upon double ionization. Since this electron-accepting orbital is antibonding between C and O, the electron flow into this orbital should result in the reduction of the C–O bond strength, thus enhancing the rupture of that bond.

The opening of the new dissociation channel leading to the ion pair $\text{FeC}^+ - \text{C}^+$ in the Fe $3p \rightarrow 3d$ photoabsorption region can also be interpreted by the same mechanism, i.e., in terms of the increase in the CO $2\pi^*$ electron density by an enhanced electron outflow from the metal d orbital. An increase in the electron population in the latter orbitals evidently should act to enhance the electron flow into the CO $2\pi^*$ orbitals through the π -back-donation orbital. A major difference of this new channel from the one following double ionization in a ligand is that the

cleavage of two C–O bonds is involved. The present model would also explain this difference consistently, since the $3p \rightarrow 3d$ photoexcitation (increase in the 3d electron population) would affect more than one ligands because the metal d orbitals interact with more than one ligands, whereas the double photoionization in one ligand can contribute to the weakening of only one C–O bond,

Summarizing, the essential factor causing breakage of covalent C–O bonds in the ligand is the enhancement of electron outflow from the metal d orbital to the CO $2\pi^*$ antibonding orbital in both cases, but the cause of this enhancement is different for different excitation/ionization processes.

Conclusion

In the present study, we have performed photoelectron–photoion coincidence (PEPICO) and photoion–photoion coincidence (PIPICO) studies of $\text{Fe}(\text{CO})_5$ in the gas phase in the photon energy range 38–120 eV to gain new insight into the dissociative photoionization processes of that compound. An emphasis has been placed on the cleavage of the covalent C–O bond. From both of the measurements, various ions and ion pairs that evidently indicate the occurrence of the C–O bond fission are observed. Almost all of them are found to originate from the doubly and triply ionized parent molecule. The ions $\text{FeC}(\text{CO})_2^+$, C^+ , and O^+ and ion pairs Fe^+-C^+ , Fe^+-O^+ , FeC^+-CO^+ , and FeC^+-O^+ sharply increase at about 42 eV, and the ion pairs FeC^+-C^+ , which can only be produced through cleavage of two C–O bonds, appear at about 60 eV. The former energy region corresponds to the double photoionization threshold of the CO ligand and the latter to the Fe $3p \rightarrow 3d$ photoabsorption limit. From these observations, we conclude that the essential factor for causing the breakage of the covalent C–O bond is the enhancement of the π -back-donation interaction, which populates the C–O antibonding orbital $2\pi^*$.

Acknowledgment. We thank the members of the UVSOR synchrotron radiation facility for their valuable assistance during the course of the experiments. This work was supported by the

Joint Studies Program of the Institute for Molecular Science. I.K. acknowledges the financial support by Grant-in-Aid for Scientific Research No. 08454189 from the Ministry of Education, Science, Culture, and Sports.

References and Notes

- (1) Armentrout, P. B. *Acc. Chem. Res.* **1995**, *28*, 430.
- (2) Winters, R. E.; Kiser, R. W. *Inorg. Chem.* **1964**, *3*, 699.
- (3) Foffani, A.; Pignataro, S.; Cantone, B.; Grasso, F. Z. *Phys. Chem. (Munich)* **1965**, *45*, 79.
- (4) Bidinosti, D. R.; McIntyre, N. S. *Can. J. Chem.* **1967**, *45*, 641.
- (5) Distifano, G. *J. Res. Natl. Bur. Stand.* **1970**, *74A*, 233.
- (6) Schultz, R. H.; Crellin, K. C.; Armentrout, P. B. *J. Am. Chem. Soc.* **1991**, *113*, 8590.
- (7) Norwood, K.; Ali, A.; Flesch, D.; Ng, C. Y. *J. Am. Chem. Soc.* **1990**, *112*, 7502.
- (8) Heck, A. J. R.; Drewello, T.; Fieber-Erdmann, M.; Weckwerth, R.; Ding, A. *J. Phys. Chem.* **1995**, *99*, 15633.
- (9) Fieber-Erdmann, M.; Holub-Kreppe, E.; Bröker, G.; Dujardin, G.; Ding, A. *Int. J. Mass Spectrom. Ion Phys.* **1995**, *149/150*, 513.
- (10) Barnes, L. A.; Rosi, M.; Bauchlicher, C. W. *J. Chem. Soc.* **1991**, *94*, 2301.
- (11) Ricca, A.; Bauchlicher, C. W. *J. Phys. Chem.* **1994**, *98*, 12899.
- (12) Ricca, A.; Bauchlicher, C. W. *J. Phys. Chem.* **1995**, *99*, 5922.
- (13) Chen, C. T. Dissertation, University of Pennsylvania, 1985.
- (14) Tamenori, Y.; Inaoka, K.; Koyano, I. *J. Electron Spectrosc. Relat. Phenom.* **1996**, *79*, 503.
- (15) Tamenori, Y.; Koyano, I. *UVSOR Activity Rep.* **1994**, *22*, 92, 94.
- (16) Tamenori, Y.; Inaoka, K.; Koyano, I. *UVSOR Activity Rep.* **1995**, *23*, 138.
- (17) (a) Tamenori, Y.; Koyano, I. *UVSOR Activity Rep.* **1995**, *23*, 140. (b) Tamenori, Y.; Koyano, I. *At. Collision Res. Jpn.* **1996**, *22*, 79.
- (18) Tamenori, Y.; Koyano, I. *UVSOR Activity Rep.* **1996**, *24*, 124.
- (19) Wen, A. T.; Rühl, E.; Hitchcock, A. P. *Organometallics* **1992**, *11*, 2559.
- (20) Hitchcock, A. P.; Wen, A. T.; Rühl, E. *Chem. Phys.* **1990**, *147*, 51.
- (21) Fronzoni, G.; Decleva, P.; Lisini, A.; Onho, M. *J. Electron Spectrosc. Relat. Phenom.* **1993**, *62*, 245.
- (22) (a) Ishiguro, E.; Suzuki, M.; Yamazaki, J.; Nakamura, E.; Sakai, K.; Matsudo, O.; Mizutani, N.; Fukui, K.; Watanabe, M. *Rev. Sci. Instrum.* **1989**, *60*, 2105 (b) Masuoka, T.; Horigome, T.; Koyano, I. *Rev. Sci. Instrum.* **1989**, *60*, 2179 (c) Masuoka, T.; Koyano, I. *J. Chem. Phys.* **1991**, *95*, 909.
- (23) Cooper, G.; Green, J. C.; Payne, M. P.; Dobson, B. R.; Hillier, I. H. *J. Am. Chem. Soc.* **1987**, *109*, 3836.
- (24) (a) Lamson, S. H.; Messner, R. P. *Phys. Rev.* **1982**, *B25*, 7209. (b) Plummer, E. W.; Chen, C. T.; Ford, W. K.; Eberhardt, W.; Messmer, R. P.; Frund, H.-J. *Surf. Sci.* **1985**, *158*, 58.
- (25) Masuoka, T.; Nakamura, E. *Phys. Rev. A* **1993**, *48*, 4379.